

Defending Against Frequency-Based Attacks with Diffusion Models

Fatemeh Amerehi Patrick Healy
Computer Science and Information Systems
University of Limerick

Fatemeh.Amerehi@ul.ie, Patrick.Healy@ul.ie

Abstract

Adversarial training is a common strategy for enhancing model robustness against adversarial attacks. However, it is typically tailored to the specific attack types it is trained on, limiting its ability to generalize to unseen threat models. Adversarial purification offers an alternative by leveraging a generative model to remove perturbations before classification. Since the purifier is trained independently of both the classifier and the threat models, it is better equipped to handle previously unseen attack scenarios. Diffusion models have proven highly effective for noise purification, not only in countering pixel-wise adversarial perturbations but also in addressing non-adversarial data shifts. In this study, we broaden the focus beyond pixel-wise robustness to explore the extent to which purification can mitigate both spectral and spatial adversarial attacks. Our findings highlight its effectiveness in handling diverse distortion patterns across low- to high-frequency regions.

1. Introduction

The accuracy of neural network predictions is often compromised by distributional shifts, whether adversarially crafted [11, 32, 80] or naturally occurring [6, 36], and whether these shifts manifest at the pixel level [58, 81] or the frequency level [24, 56].

Pixel-wise adversarial attacks are designed to be minimally detectable, leveraging subtle perturbations to mislead models while preserving visual similarity [32]. Their imperceptibility is typically measured using ℓ_p norms [13, 16, 46, 58, 61] and, in some cases, human perception [24, 55, 71, 95].

These perturbations are typically crafted through an optimization process to maximize the model’s loss and are then added to the original input [45, 46, 58, 63]. The Fast Gradient Sign Method (FGSM) [32] approximates this maximization by performing a single gradient step to identify the direction in which the loss increases most rapidly. Iterative extensions, such as the Basic Iterative Method [45] and

Projected Gradient Descent (PGD) [58], strengthen FGSM by applying multiple iterations to refine the adversarial perturbation. AutoAttack [21] further advances these techniques by combining two parameter-free PGD variants with the Fast Adaptive Boundary attack [20] and the Square Attack [3], enabling both white-box and black-box attacks.

Frequency-based attacks modify images by adjusting energy in specific frequency bands [24, 43, 56]. This often involves transforming the image into the frequency domain, making subtle modifications, and then converting it back, all while preserving visual quality and minimizing perceptible noise [38, 72]. AdvDrop [29] removes features essential to the model yet unnoticeable to human observers by quantitatively reducing targeted frequency components [29].

Frequency-domain filtering constrains perturbations to high-frequency components [56] or narrows the search for adversarial images to low-frequency regions [34]. Frequency-selective attacks independently manipulate amplitude and phase components, enabling more precise control over perturbations [43]. Some methods introduce large perturbation magnitudes [38], while others accelerate feature collapse in vision transformers [26] by exploiting their reliance on low-frequency components [30]. F-mixup [51] generates adversarial examples by blending the low-frequency component of one class with the high-frequency component of another. Frequency Dropout [96] reduces certain gradient frequency coefficients to improve attack transferability, assuming that high-frequency components contain noise and overfitting details related to the substitute model. AdvINN [16] utilizes Discrete Wavelet Transform to decompose the clean and target images into low- and high-frequency components. It then generates adversarial samples by exchanging feature-level information, suppressing discriminative details in the clean images, and embedding class-specific attributes from the target samples.

Beyond these methods, other attack strategies employ generative models [15, 39], alter pixel positions [89], or leverage transformations such as subtly modifying shape [89], as well as modifying texture and color [1, 10, 71], or combining all of these within the image content [17].

In response, various defense mechanisms exist, including defensive distillation [68], feature squeezing [91], logit pairing [41], adversarial detection [59, 67], gradient regularization [83, 88], adversarial training [32, 58, 87], and adversarial purification [50, 53, 65, 92].

Among these approaches, adversarial training has been shown to be highly effective [5, 8, 12, 32, 45, 63]. However, it often comes with a trade-off between robustness and accuracy [84, 94], as well as between in- and out-of-distribution generalization [94]. It can also interfere with a model’s invariance to input transformations [40, 73], while amplifying performance disparities across different classes [9, 57]. Moreover, adversarial training shows limited generalization to unseen attacks [47, 79]. While models exhibit robustness against the specific threat model they were trained on, they often remain vulnerable to others [82]. For example, models trained with ℓ_∞ threat models may lack robustness to ℓ_2 or spatial adversarial perturbations, and vice versa [65].

Unlike adversarial training, adversarial purification uses a generative model to remove adversarial perturbations from images prior to classification [92]. This approach offers greater flexibility, as the purification models are trained independently without any assumptions about the attack type or classifier, making them effective against a wide range of previously unseen adversarial perturbations [65]. The use of diffusion models [25, 37, 77] for noise purification has proven highly effective in countering pixel-wise adversarial perturbations, consistently outperforming adversarial training in ℓ_∞ and ℓ_2 threat models [65], as well as in certified adversarial robustness [14]. Moreover, their effectiveness extends beyond adversarial robustness to broader data shifts, including variations in style [93], as well as non-adversarial perturbations [31]. Moving beyond pixel-wise robustness, this paper broadens the lens and provides insight into how purification handles shifts in both spatial and spectral domains.

2. Related Works

Having explored adversarial attacks, the following section reviews literature on methods for addressing unseen attack scenarios and adversarial purification techniques.

Robustness Against Unforeseen Attacks. Many defense mechanisms offer guarantees based on specific threat models [19] or integrate knowledge of the threat model during training [58]. Adversarial training, while effective against known threats, primarily relies on generated perturbations and thus struggles to generalize to unseen attacks. It typically assumes the adversary follows a predefined threat model, such as ℓ_p -bounded perturbations within a fixed budget, which may not always hold true [47].

One approach to mitigating unseen threats involves generating adversarial examples for all types of perturbations

and training on either all of these examples or focusing on the worst-case scenario [82]. Dual Manifold Adversarial Training leverages information about the underlying manifold of natural images, employing adversarial perturbations in both the latent and image spaces, enabling generalization to both ℓ_p -bounded and non-norm-bounded threats. Variation Regularization reduces the variation in the feature extractor across the source threat model during training, improving the model’s ability to generalize to previously unseen attacks [22]. Confidence-calibrated adversarial training introduces a target distribution that favors uniformity for large perturbations, allowing the model to extrapolate beyond the threat model employed during training [79]. Additionally, some methods offer bounds for generalizing to an unknown adversary with oracle access during training [62].

Adversarial purification. Adversarial purification employs a standalone model that removes adversarial noise from potentially attacked images, restoring them to a clean state for classification [65, 76, 78, 92]. Defense-GAN [70] leverages Wasserstein GANs [4] to model the distribution of unperturbed images and, during inference, reconstructs an image free of adversarial perturbations by finding a latent vector that minimizes the difference between the generated and input images, which is then classified [70]. PixelDefend [76] utilizes the autoregressive generative model PixelCNN [85] to detect and purify adversarial examples. Some approaches employ energy-based models [28, 33, 78] to purify attacked images through Langevin dynamics, while others rely on denoising score-based generative models [75, 92]. DiffPure [65] uses diffusion models to purify adversarial examples prior to inputting them into classifiers. A guided diffusion model for adversarial purification employs the difference between an adversarial example and a purified one as a form of guidance [86]. Alternatively, it may utilize an auxiliary neural network, trained through adversarial learning, to steer the reverse diffusion process based on latent representation distances rather than pixel-level values [53]. Another approach involves the use of contrastive guidance [7].

DensePure [90] performs multiple denoising steps with different random seeds to generate reversed samples, which are then classified and combined through majority voting for the final prediction. Other methods use random transforms to prevent overfitting to known attacks and fine-tune the purifier model with adversarial loss to enhance robustness [52], or adopt a gradual noise-scheduling strategy to strengthen diffusion-based purification [48]. While these works primarily investigate pixel-wise adversarial perturbations in the spatial domain, we redirect the focus toward frequency-based perturbations in the spectral domain, as it remains a less-studied aspect of adversarial purification and robustness.



Figure 1. Clean, adversarial, diffused, and purified images. The clean image is the original, uncorrupted image from ImageNet. The adversarial image is generated for ResNet-50 by perturbing all components (magnitude, phase, and pixel values) of the image. The adversarial image is then purified using diffusion purification. The diffused image corresponds to $t^* = 0.15$, and the purified image is obtained at $t = 0$.

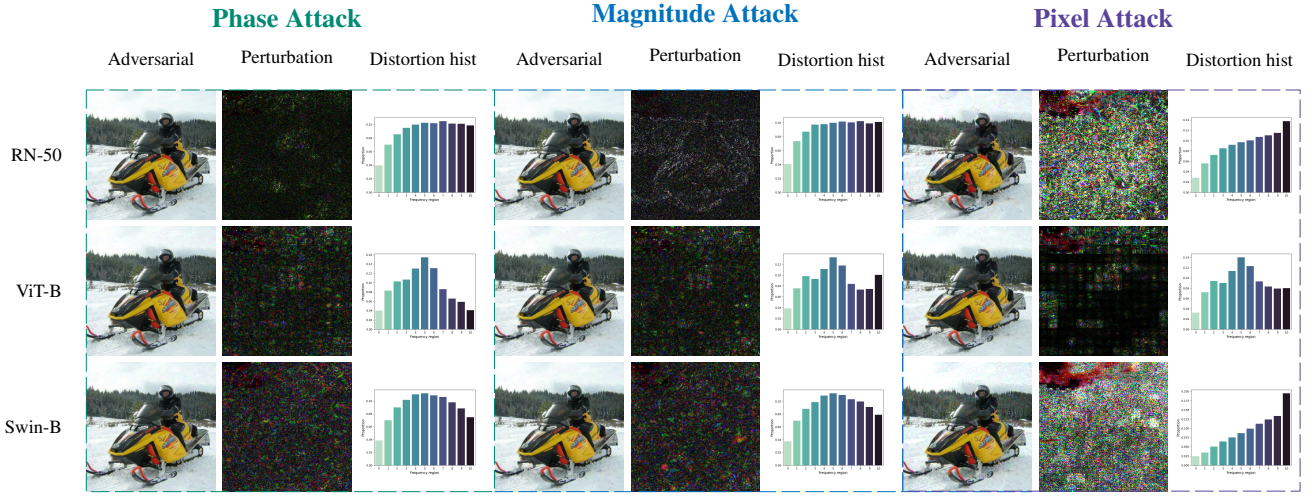


Figure 2. Adversarial examples generated by perturbing the magnitude, phase, and pixel values across various architectures. The perturbations, representing the differences between the original and attacked images (magnified by a factor of 20 for visualization). The distortion histograms, obtained by applying the Fourier transform to the perturbations, highlight the impact of each attack on the spectral characteristics of the images. In ResNet-50 [35], the distortion is primarily concentrated in high-frequency regions, while ViT-B [27] and Swin-B [54] exhibit distortions mainly in the mid-to-low frequency ranges.

3. Attack and Defense Mechanisms

In this section, we provide a detailed description of the attack method and the purification technique used.

3.1. Frequency-Based Attacks

Targeting different image components creates distinct distortion patterns within the image, which also vary depending on the chosen model. Figure 2 illustrates various attack distortion patterns by perturbing the pixel values, phase, amplitude, or a combination of these elements in a clean image (leftmost in Figure 1), as described below.

An image x in the spatial domain can be represented in the frequency domain through the Discrete Fourier Transform (DFT) [18], which decomposes the image into its frequency components. The Fourier transform of an image x can be expressed as:

$$\mathcal{F}\{x\} = M \cdot e^{i\phi}, \quad (1)$$

where M and ϕ represent the magnitude (amplitude) and phase spectra, respectively. Following [43], to generate an adversarially perturbed image x' , we apply a combination of multiplicative magnitude perturbation δ_{mag} , additive phase perturbation δ_{phase} , and additive pixel perturbation δ_{pixel} . The perturbed image x' is thus given by:

$$\tilde{x}' = \mathcal{F}^{-1} \left(\text{clip}_{0,\infty} (M \otimes \delta_{\text{mag}}) \cdot e^{i(\phi + \delta_{\text{phase}})} \right) + \delta_{\text{pixel}}, \quad (2)$$

where \mathcal{F}^{-1} denotes the inverse Fourier transform, \otimes represents element-wise multiplication, and $\text{clip}_{0,\infty}$ truncates the values of the magnitude spectrum within the range $[0, \infty)$. The image \tilde{x}' is the intermediate image obtained after the inverse Fourier transform.

To ensure that the pixel values remain within the valid range $[0, 1]$, the resulting image is clipped as follows:

$$x' = \text{clip}_{0,1} (\tilde{x}'), \quad (3)$$

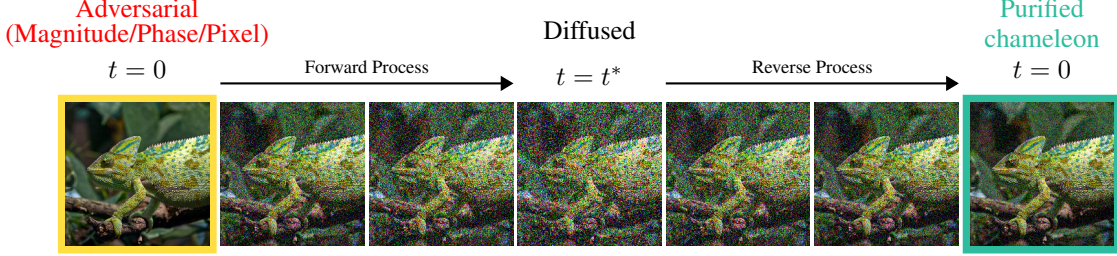


Figure 3. Diffusion-driven purification introduces noise to adversarial images by following the forward diffusion process with a small diffusion timestep t^* to obtain the diffused images. These images are then denoised through the reverse denoising process to recover the clean images before classification.

The magnitude perturbation δ_{mag} modifies the strength of the frequency components, while the phase perturbation δ_{phase} alters the spatial alignment, resulting in structural changes that may not be visually perceptible. The term δ_{pixel} represents an additive perturbation in the spatial domain.

To maintain real-valued pixel outputs from the inverse Fourier transform, the perturbations δ_{mag} and δ_{phase} are kept symmetric. Adversarial attacks can be performed using a single perturbation δ_{mag} , δ_{phase} , or δ_{pixel} , which we refer to as a magnitude attack, phase attack, and pixel attack, respectively. Additionally, combinations of multiple perturbations are possible, which we also explore in this work.

To obtain the adversarial image x' , the perturbations are optimized via gradient descent. To limit distortion (for imperceptibility) while maximizing the cross-entropy loss and thereby misleading the classifier, the optimization process minimizes the ℓ_2 difference between the original and perturbed images. The loss function is formulated as:

$$\mathcal{L} = \lambda \cdot \ell_2(x', x) - \sum_k y_k \log f_k(x') \quad (4)$$

where λ is a balancing parameter that controls the trade-off between distortion and classification loss. Here, $f_k(x')$ represents the classifier's predicted probability for class k , and y is the one-hot ground truth label.

3.2. Diffusion-Driven Purification Defense

Here, we first overview continuous-time diffusion models, followed by the diffusion purification method used.

Continuous-Time Diffusion Models. Diffusion-based probabilistic generative models operate by progressively corrupting training data with noise and then learning to reverse this corruption, effectively modeling the underlying data distribution [25, 37, 75, 77]. Denoising Diffusion Probabilistic Models (DDPMs) learn to generate data by reversing a Markovian diffusion process that maps complex data distributions to a simple prior, typically an isotropic Gaussian, refining noise into structured samples [37, 64, 74]. Instead of applying noise in discrete steps, continuous-time diffusion models use stochastic differential equations

(SDEs) to gradually transform data into noise and vice versa [77]. Formally, given the unknown data distribution $p(x)$ from which each data point $x \in \mathbb{R}^d$ is sampled, the diffusion process gradually transitions $p(x)$ towards a noise distribution. The forward diffusion process $\{x(t)\}_{t \in [0,1]}$, can be described by the following stochastic differential equation:

$$dx = h(x, t)dt + g(t)dw, \quad (5)$$

where $x(0) := x \sim p(x)$, $h : \mathbb{R}^d \times \mathbb{R} \rightarrow \mathbb{R}^d$ represents the drift coefficient, $g : \mathbb{R} \rightarrow \mathbb{R}$ is the diffusion coefficient, and $w(t) \in \mathbb{R}^n$ is the standard Wiener process (a.k.a., Brownian motion). Under suitable conditions conditions [2, 77], the reverse process exists and undo the added noise by solving the reverse-time SDE:

$$d\hat{x} = [h(\hat{x}, t) - g(t)^2 \nabla_{\hat{x}} \log p_t(\hat{x})] dt + g(t)d\bar{w}, \quad (6)$$

where $d\bar{w}$ represents the reverse-time standard Wiener process, and $\nabla_x \log p_t(x)$ denotes the time-dependent score function. Following the conventions of the variance-preserving stochastic differential equation (VP-SDE) [77], the drift and diffusion terms are given by

$$h(x; t) = -\frac{1}{2}\beta(t)x, \quad g(t) = \sqrt{\beta(t)}, \quad (7)$$

with $\beta(t)$ representing a time-dependent noise scale, which is positive and continuous over the interval $[0, 1]$, such that the state at time t can be rewritten as:

$$x(t) = \sqrt{\alpha_t}x(0) + \sqrt{1 - \alpha_t}\epsilon, \quad (8)$$

where $\alpha_t = e^{-\int_0^t \beta(s)ds}$, and $\epsilon \sim \mathcal{N}(0, I)$. We denote the reverse-SDE by $\{\hat{x}_t\}_{t \in [0,1]}$ from Eq. 6, which follows the same distribution as the forward-SDE $\{x_t\}_{t \in [0,1]}$ from Eq. 5.

Diffusion-Driven Adversarial Purification. Similar to [65], we employ a two-step adversarial purification method. We begin with an adversarial example $x' = x(0)$ at

time $t = 0$ and remove its noise through a diffusion model. The first step involves diffusing the input by solving a forward SDE, as given in Eq. 5, which gradually adds noise from $t = 0$ to $t = t^*$. Specifically, for a chosen diffusion timestep $t \in [0, 1]$, the diffused sample is obtained from Eq. 8. Once the adversarial input has been sufficiently diffused, we reverse the process by solving the reverse SDE in Eq. 6 from $t = t^*$ to obtain a purified input $\hat{x}(0)$. This purified input is subsequently passed to a standard classifier for prediction. This is illustrated in Figure 3. Examples of clean, pixel-attacked, diffused, and purified images are shown in Figure 4.

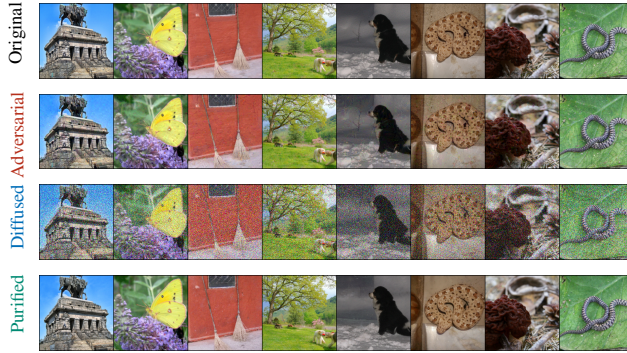


Figure 4. Example of purified images for a pixel attack on the ResNet-50 model with $t^* = 0.15$.

4. Experimental Setup

Below, we detail the dataset, training configuration, employed networks, and evaluation metrics, followed by the presentation of results and analysis.

4.1. Configurations and Metrics

We aim to explore the effectiveness of adversarial purification against perturbations in the spatial and spectral domains across multiple pre-trained classifier architectures. Specifically, we evaluate ResNet-50 [35] as a CNN, ViT-B-16 [27] as a transformer model, and Swin-B [54] as a hybrid architecture for a comprehensive evaluation on ImageNet [23] dataset.

We minimize the loss in Eq. 4 using the Adam optimizer [44] with a fixed learning rate of 5×10^{-3} and a weight decay of 5×10^{-6} . The optimization is performed for a maximum of 1000 iterations, with a termination condition that halts the process if the loss does not improve over five consecutive iterations. To control the attack strength, we use the value of $\lambda = 5 \times 10^4$, which is the default setting employed by [43].

For diffusion purification, we follow the experimental setup in [65]. Specifically, we use the adjoint framework for SDEs provided by the TorchSDE library [42, 49] for

both adversarial purification and gradient evaluation. Both SDEs are solved using the simple Euler-Maruyama method with a fixed step size of $dt = 10^{-3}$. Additionally, we use the 256×256 unconditional diffusion checkpoint from the Guided Diffusion library [66].

Evaluation metrics. We evaluate models using both standard and robust accuracy. In Tables 3 and 4, "Clean (No Attack)" represents the performance of the pretrained classifier on the entire test set of clean ImageNet data, without any purification. Similarly, "Adversarial" denotes the performance of the model on adversarial examples generated from spectral and spatial attacks. The "Purified Clean" refers to the accuracy of the pretrained classifier on clean test samples that have been processed through the diffusion model for purification before classification. This metric allows us to assess the impact of purification on clean accuracy and analyze the trade-off between improved robustness and potential accuracy loss on unperturbed samples. The "Adversarial Purified" measures the classifier's performance on adversarial examples (from spectral and spatial attacks) that are first processed through the diffusion model for purification before classification. Following [65], adversarial accuracies are evaluated on a fixed subsets of 512 randomly sampled images. Specifically, we use three subsets, each containing 512 samples, and each experiment is repeated three times. The results are reported as the mean and standard deviation.

We also compare the trade-off between the clean accuracy of the pre-trained model and the clean accuracy achieved through adversarial training and diffusion purification, evaluated on a fixed subset of 512 randomly sampled images from the test set. The adversarially trained model is chosen to be robust against AutoAttack ($\varepsilon = 4/255$, ℓ_∞) from RobustBench [21]. Specifically, for ResNet-50 [35], we use the adversarially trained model from [69], and for ViT-B-16 [27] and Swin-B [54], we use the models from [60]. For purification, the diffusion timestep is set to $t^* = 0.15$. Additionally, to evaluate the effect of diffusion timestep, we consider $t^* = 0.1$ and $t^* = 0.125$.

5. Results

Figure 2 clearly illustrates that different models generate distinct distortion patterns. Moreover, perturbing various image components (pixel, phase, and amplitude) within the same model also leads to differing distortion patterns (both high and low frequency). To better understand how purification handles these diverse distortion patterns, Table 3 presents the performance of diffusion purification across various adversarial perturbations applied to different network architectures.

The pixel attack is most effective on the ResNet-50 model, and purification effectively restores the adversarial sample, enhancing its robustness. Similarly, for spectral at-

tacks, diffusion purification is highly effective at removing perturbations. On average, across both spatial and spectral perturbations, the robustness improves by up to $7.72 \times 10^2\%$ compared to the pre-trained model. In terms of clean accuracy, there is an average drop of 8.62% across all perturbations compared to the pre-trained model, due to the clean input passing through adversarial purification. This drop is typically not reported in previous studies [65]; however, in real-world scenarios, we do not know in advance which samples are clean and which are adversarially crafted. Although clean accuracy decreases, as shown in Table 1, purification still results in a smaller trade-off, and offering better robustness compared to adversarial training. Similarly, for the ViT and Swin-B models, adversarial perturbations degrade performance in both spectral and spatial domains, but purification results in significant benefits, even more so than for the CNN model. In terms of robustness, although there is a clean accuracy drop of 5.60% for ViT and 6.79% for Swin-B on average across all perturbations due to purifying clean samples, the robustness gain is as high as $8.20 \times 10^3\%$ for ViT and $7.73 \times 10^5\%$ for Swin-B compared to the pre-trained model after purification.

Table 1 presents the trade-off between the clean accuracy of the pre-trained models and the clean accuracy achieved through adversarial training [84, 94] and diffusion purification. While both adversarial training and diffusion purification reduce the clean accuracy of the pre-trained model across all models, diffusion purification incurs less accuracy loss and achieves superior robustness compared to adversarial training [65].

Table 2 compares the performance of robust adversarially trained models against unseen frequency perturbations and purification. On average, across all perturbations, the performance gain with purification is 66.49% for the ResNet-50 model, compared to adversarial training, and 15.97% for the ViT model.

Table 4 compares the impact of diffusion timestep t^* . For the ResNet-50 model, across all perturbations, a smaller timestep $t^* = 0.1$ results in better clean accuracy, while larger diffusion timesteps enhance adversarial robustness. In the case of the ViT-b model, the timestep has a relatively minor effect, with similar performance observed across various timesteps $t^* = 0.1$, $t^* = 0.125$, and $t^* = 0.15$ (as shown in Table 3). For the Swin-b model, a smaller t^* achieves better adversarial gains.

6. Conclusions

In this study, we employed the Diffusion model to evaluate the effectiveness of purification in countering diverse adversarial perturbations across both spectral and spatial domains. Our findings consistently demonstrate the model's robustness across all tested scenarios, emphasizing that purification is highly effective in restoring robustness against

unseen and varied adversarial perturbations while incurring minimal trade-offs.

Model	Clean (Pre-trained)	Clean (Robust)	Clean (Purified)
ResNet-50 (Salman et al., 2020) [69]	75.78	63.86	70.89
ViT-B (Mo et al., 2022) [60]	82.61	67.77	77.73
Swin-B (Mo et al., 2022) [60]	84.76	74.8	81.05

Table 1. Clean accuracy trade-off between purification and adversarially trained models on ImageNet under AutoAttack ($\epsilon = 4/255$, ℓ_∞). Adversarially trained models are sourced from RobustBench [21], while purification is applied with a diffusion timestep of $t^* = 0.15$. Clean (Pre-trained), Clean (Robust), and Clean (Purified) refer to the clean accuracy of the pre-trained model, adversarially trained model, and purified AutoAttack [21] examples, respectively. Adversarial purification leads to smaller reductions in clean accuracy while achieving greater improvements in robustness (Tables 3 and 2 and [65]).

	Accuracy		
	Adversarial		Purified
			Adversarial
ResNet-50 (Salman et al., 2020) [69]	Pixel	29.49	63.86
	Mag	48.05	68.75
	Phase	49.61	67.77
	Phase+Mag	41.02	66.61
	All	29.49	64.06
	Mean	39.53	66.21
ViT-B-16 (Mo et al., 2022) [60]	Pixel	63.28	74.02
	Mag	65.42	76.37
	Phase	66.01	75.19
	Phase+Mag	63.67	73.44
	All	63.08	73.82
	Mean	64.29	74.56

Table 2. Comparison of the robustness of purification and adversarially trained models against frequency-based perturbations. Adversarial purification shows superior robustness in countering frequency attacks.

Acknowledgments

This publication has emanated from research conducted with the financial support of Taighde Éireann – Research Ireland under Grant No. 18/CRT/6223.

		Accuracy			
		Clean (No Attack)	Adversarial	Purified Clean	Purified Adversarial
ResNet-50	pixel	76.69 \pm 1.12	1.17 \pm 0.35	70.08 \pm 0.96	64.29 \pm 1.48
	mag	76.69 \pm 1.12	12.96 \pm 1.62	70.08 \pm 0.96	67.06 \pm 1.23
	phase	76.69 \pm 1.12	12.73 \pm 1.54	70.12 \pm 1.00	67.02 \pm 1.70
	phase+mag	76.69 \pm 1.12	9.70 \pm 1.47	70.05 \pm 0.98	65.27 \pm 0.92
	all	76.69 \pm 1.12	1.04 \pm 0.27	70.08 \pm 0.96	64.26 \pm 1.32
	mean	76.69 \pm 1.04	7.52 \pm 5.57	70.08 \pm 0.90	65.58 \pm 1.79
ViT-B-16	pixel	80.47 \pm 1.68	0.16 \pm 0.15	75.98 \pm 1.22	74.54 \pm 1.86
	mag	80.47 \pm 1.68	1.89 \pm 0.34	75.98 \pm 1.22	74.71 \pm 1.69
	phase	80.47 \pm 1.68	1.92 \pm 0.23	75.94 \pm 1.21	75.03 \pm 1.65
	phase+mag	80.47 \pm 1.68	0.46 \pm 0.24	75.98 \pm 1.22	74.74 \pm 1.59
	all	80.47 \pm 1.68	0.07 \pm 0.10	75.94 \pm 1.21	74.67 \pm 1.76
	mean	80.47 \pm 1.56	0.90 \pm 0.87	75.96 \pm 1.13	74.74 \pm 1.60
Swin-B	pixel	84.57 \pm 0.46	0.07 \pm 0.10	78.84 \pm 1.38	77.31 \pm 1.04
	mag	84.57 \pm 0.46	0.00 \pm 0.00	78.81 \pm 1.36	77.34 \pm 0.95
	phase	84.57 \pm 0.46	0.00 \pm 0.00	78.84 \pm 1.38	77.41 \pm 0.77
	phase+mag	84.57 \pm 0.46	0.00 \pm 0.00	78.84 \pm 1.38	77.41 \pm 0.67
	all	84.57 \pm 0.46	0.00 \pm 0.00	78.81 \pm 1.36	77.25 \pm 1.02
	mean	84.57 \pm 0.43	0.01 \pm 0.05	78.83 \pm 1.28	77.34 \pm 0.84

Table 3. Performance of diffusion purification on various types of adversarial perturbations across different networks on ImageNet. "Clean (No Attack)" and "Adversarial" denote classifier performance on clean and adversarial examples without purification. "Purified Clean" and "Adversarial Purified" assess accuracy on clean and adversarial samples after purification using diffusion timesteps $t^* = 0.15$. Purification enhances robustness across various perturbations and models, with notable improvements in both pixel and spectral attacks. While clean accuracy drops slightly due to the purification process, robustness gains are substantial, particularly for ViT and Swin-B models.

References

- [1] Mahmoud Afifi and Michael S Brown. What else can fool deep learning? addressing color constancy errors on deep neural network performance. In *Proceedings of the IEEE/CVF international conference on computer vision*, pages 243–252, 2019. 1
- [2] Brian DO Anderson. Reverse-time diffusion equation models. *Stochastic Processes and their Applications*, 12(3):313–326, 1982. 4
- [3] Maksym Andriushchenko, Francesco Croce, Nicolas Flammarion, and Matthias Hein. Square attack: a query-efficient black-box adversarial attack via random search. In *European conference on computer vision*, pages 484–501. Springer, 2020. 1
- [4] Martin Arjovsky, Soumith Chintala, and Léon Bottou. Wasserstein generative adversarial networks. In *Proceedings of the 34th International Conference on Machine Learning*, pages 214–223. PMLR, 2017. 2
- [5] Anish Athalye, Nicholas Carlini, and David Wagner. Obfuscated gradients give a false sense of security: Circumventing
- defenses to adversarial examples. In *International conference on machine learning*, pages 274–283. PMLR, 2018. 2
- [6] Aharon Azulay and Yair Weiss. Why do deep convolutional networks generalize so poorly to small image transformations? *arXiv preprint arXiv:1805.12177*, 2018. 1
- [7] Mingyuan Bai, Wei Huang, Tenghui Li, Andong Wang, Junbin Gao, César Federico Caiafa, and Qibin Zhao. Diffusion models demand contrastive guidance for adversarial purification to advance. 2024. 2
- [8] Tao Bai, Jinqi Luo, Jun Zhao, Bihang Wen, and Qian Wang. Recent advances in adversarial training for adversarial robustness. In *Proceedings of the Thirtieth International Joint Conference on Artificial Intelligence, IJCAI-21*, pages 4312–4321. International Joint Conferences on Artificial Intelligence Organization, 2021. Survey Track. 2
- [9] Philipp Benz, Chaoning Zhang, Adil Karjauv, and In So Kweon. Robustness may be at odds with fairness: An empirical study on class-wise accuracy. In *NeurIPS 2020 Workshop on pre-registration in machine learning*, pages 325–342. PMLR, 2021. 2

		Accuracy					
		Clean (No Attack)	Adversarial	$t^* = 0.125$	$t^* = 0.1$	Purified Clean	Purified Adversarial
				$t^* = 0.125$	$t^* = 0.1$	$t^* = 0.125$	$t^* = 0.1$
ResNet-50	pixel	78.13	1.56	72.66	73.05	65.43	61.72
	mag	78.13	10.94	72.66	73.05	66.02	65.63
	phase	78.13	12.89	72.66	73.05	67.38	68.16
	phase+mag	78.13	7.62	72.66	73.05	63.48	60.94
	all	78.13	1.95	72.66	73.05	64.65	60.74
	mean	78.13	6.99	72.66	73.05	65.39	63.44
ViT-B-16	pixel	79.10	0.00	76.56	75.78	75.00	74.61
	mag	79.10	1.76	76.56	75.78	74.22	73.83
	phase	79.10	2.34	76.56	75.78	75.00	74.41
	phase+mag	79.10	0.20	76.56	75.78	75.20	73.63
	all	79.10	0.00	76.56	75.78	74.80	74.80
	mean	79.10	0.86	76.56	75.78	74.84	74.26
Swin-B	pixel	84.96	0.00	78.32	80.27	78.91	78.91
	mag	84.96	0.00	78.32	80.27	78.91	78.71
	phase	84.96	0.00	78.32	80.27	79.10	80.08
	phase+mag	84.96	0.20	78.32	80.27	77.93	78.71
	all	84.96	0.00	78.32	80.27	78.71	80.66
	mean	84.96	0.02	78.32	80.27	78.71	79.41

Table 4. The impact of diffusion timestep t^* on the performance of diffusion purification across various perturbations and networks on ImageNet. Overall, larger diffusion timesteps enhance robustness, while smaller timesteps yield better clean accuracy, although they reduce the effectiveness of adversarial purification.

- [10] Anand Bhattacharjee, Min Jin Chong, Kaizhao Liang, Bo Li, and D. A. Forsyth. Unrestricted adversarial examples via semantic manipulation. In *International Conference on Learning Representations*, 2020. 1
- [11] Battista Biggio, Igino Corona, Davide Maiorca, Blaine Nelson, Nedim Šrndić, Pavel Laskov, Giorgio Giacinto, and Fabio Roli. Evasion attacks against machine learning at test time. In *Machine learning and knowledge discovery in databases: European conference, ECML PKDD 2013, prague, czech Republic, September 23-27, 2013, proceedings, part III I3*, pages 387–402. Springer, 2013. 1
- [12] Nicholas Carlini and David Wagner. Adversarial examples are not easily detected: Bypassing ten detection methods. In *Proceedings of the 10th ACM workshop on artificial intelligence and security*, pages 3–14, 2017. 2
- [13] Nicholas Carlini and David Wagner. Towards evaluating the robustness of neural networks. In *2017 ieee symposium on security and privacy (sp)*, pages 39–57. Ieee, 2017. 1
- [14] Nicholas Carlini, Florian Tramer, Krishnamurthy Dj Dvijotham, Leslie Rice, Mingjie Sun, and J Zico Kolter. (certified!!) adversarial robustness for free! In *The Eleventh International Conference on Learning Representations*, 2023. 2
- [15] Xinquan Chen, Xitong Gao, Juanjuan Zhao, Kejiang Ye, and Cheng-Zhong Xu. Advdiffuser: Natural adversarial example synthesis with diffusion models. In *Proceedings of the IEEE/CVF International Conference on Computer Vision*, pages 4562–4572, 2023. 1
- [16] Zihan Chen, Ziyue Wang, Jun-Jie Huang, Wentao Zhao, Xiao Liu, and Dejian Guan. Imperceptible adversarial attack via invertible neural networks. In *Proceedings of the AAAI Conference on Artificial Intelligence*, pages 414–424, 2023. 1
- [17] Zhaoyu Chen, Bo Li, Shuang Wu, Kaixun Jiang, Shouhong Ding, and Wenqiang Zhang. Content-based unrestricted adversarial attack. *Advances in Neural Information Processing Systems*, 36, 2024. 1
- [18] James W Cooley and John W Tukey. An algorithm for the machine calculation of complex fourier series. *Mathematics of computation*, 19(90):297–301, 1965. 3
- [19] Francesco Croce and Matthias Hein. Provable robustness against all adversarial l_p -perturbations for $p \geq 1$. In *International Conference on Learning Representations*, 2020. 2
- [20] Francesco Croce and Matthias Hein. Minimally distorted adversarial examples with a fast adaptive boundary attack.

- In *International Conference on Machine Learning*, pages 2196–2205. PMLR, 2020. 1
- [21] Francesco Croce and Matthias Hein. Reliable evaluation of adversarial robustness with an ensemble of diverse parameter-free attacks. In *International conference on machine learning*, pages 2206–2216. PMLR, 2020. 1, 5, 6
- [22] Sihui Dai, Saeed Mahloujifar, and Prateek Mittal. Formulating robustness against unforeseen attacks. *Advances in Neural Information Processing Systems*, 35:8647–8661, 2022. 2
- [23] Jia Deng, Wei Dong, Richard Socher, Li-Jia Li, Kai Li, and Li Fei-Fei. Imagenet: A large-scale hierarchical image database. In *2009 IEEE conference on computer vision and pattern recognition*, pages 248–255. Ieee, 2009. 5
- [24] Yingpeng Deng and Lina J Karam. Frequency-tuned universal adversarial perturbations. In *Computer Vision–ECCV 2020 Workshops: Glasgow, UK, August 23–28, 2020, Proceedings, Part V 16*, pages 494–510. Springer, 2020. 1
- [25] Prafulla Dhariwal and Alexander Nichol. Diffusion models beat gans on image synthesis. *Advances in neural information processing systems*, 34:8780–8794, 2021. 2, 4
- [26] Yihe Dong, Jean-Baptiste Cordonnier, and Andreas Loukas. Attention is not all you need: Pure attention loses rank doubly exponentially with depth. In *International conference on machine learning*, pages 2793–2803. PMLR, 2021. 1
- [27] Alexey Dosovitskiy, Lucas Beyer, Alexander Kolesnikov, Dirk Weissenborn, Xiaohua Zhai, Thomas Unterthiner, Mostafa Dehghani, Matthias Minderer, Georg Heigold, Sylvain Gelly, Jakob Uszkoreit, and Neil Houlsby. An image is worth 16x16 words: Transformers for image recognition at scale. In *International Conference on Learning Representations*, 2021. 3, 5
- [28] Yilun Du and Igor Mordatch. Implicit generation and modeling with energy based models. *Advances in neural information processing systems*, 32, 2019. 2
- [29] Ranjie Duan, Yuefeng Chen, Dantong Niu, Yun Yang, A Kai Qin, and Yuan He. Advdrop: Adversarial attack to dnns by dropping information. In *Proceedings of the IEEE/CVF International Conference on Computer Vision*, pages 7506–7515, 2021. 1
- [30] Chenxing Gao, Hang Zhou, Junqing Yu, YuTeng Ye, Jiale Cai, Junle Wang, and Wei Yang. Attacking transformers with feature diversity adversarial perturbation. In *Proceedings of the AAAI Conference on Artificial Intelligence*, pages 1788–1796, 2024. 1
- [31] Jin Gao, Jialing Zhang, Xihui Liu, Trevor Darrell, Evan Shethamer, and Dequan Wang. Back to the source: Diffusion-driven adaptation to test-time corruption. In *Proceedings of the IEEE/CVF Conference on Computer Vision and Pattern Recognition*, pages 11786–11796, 2023. 2
- [32] Ian J Goodfellow, Jonathon Shlens, and Christian Szegedy. Explaining and harnessing adversarial examples. *arXiv preprint arXiv:1412.6572*, 2014. 1, 2
- [33] Will Grathwohl, Kuan-Chieh Wang, Joern-Henrik Jacobsen, David Duvenaud, Mohammad Norouzi, and Kevin Swersky. Your classifier is secretly an energy based model and you should treat it like one. In *International Conference on Learning Representations*, 2020. 2
- [34] Chuan Guo, Jared S Frank, and Kilian Q Weinberger. Low frequency adversarial perturbation. *Machine Learning research*, 2018. 1
- [35] Kaiming He, Xiangyu Zhang, Shaoqing Ren, and Jian Sun. Deep residual learning for image recognition. In *Proceedings of the IEEE conference on computer vision and pattern recognition*, pages 770–778, 2016. 3, 5
- [36] Dan Hendrycks and Thomas Dietterich. Benchmarking neural network robustness to common corruptions and perturbations. In *International Conference on Learning Representations*, 2019. 1
- [37] Jonathan Ho, Ajay Jain, and Pieter Abbeel. Denoising diffusion probabilistic models. *Advances in neural information processing systems*, 33:6840–6851, 2020. 2, 4
- [38] Jiaxing Huang, Dayan Guan, Aoran Xiao, and Shijian Lu. Rda: Robust domain adaptation via fourier adversarial attacking. In *Proceedings of the IEEE/CVF international conference on computer vision*, pages 8988–8999, 2021. 1
- [39] Ajil Jalal, Andrew Ilyas, Constantinos Daskalakis, and Alexandros G Dimakis. The robust manifold defense: Adversarial training using generative models. *arXiv preprint arXiv:1712.09196*, 2017. 1
- [40] Sandesh Kamath, Amit Deshpande, Subrahmanyam Kambhampati Venkata, and Vineeth N Balasubramanian. Can we have it all? on the trade-off between spatial and adversarial robustness of neural networks. *Advances in Neural Information Processing Systems*, 34:27462–27474, 2021. 2
- [41] Harini Kannan, Alexey Kurakin, and Ian Goodfellow. Adversarial logit pairing. *arXiv preprint arXiv:1803.06373*, 2018. 2
- [42] Patrick Kidger, James Foster, Xuechen Li, Harald Oberhauser, and Terry Lyons. Neural SDEs as Infinite-Dimensional GANs. *International Conference on Machine Learning*, 2021. 5
- [43] Gihyun Kim, Juyeop Kim, and Jong-Seok Lee. Exploring adversarial robustness of vision transformers in the spectral perspective. In *Proceedings of the IEEE/CVF Winter Conference on Applications of Computer Vision*, pages 3976–3985, 2024. 1, 3, 5
- [44] Diederik P Kingma and Jimmy Ba. Adam: A method for stochastic optimization. *arXiv preprint arXiv:1412.6980*, 2014. 5
- [45] Alexey Kurakin, Ian Goodfellow, and Samy Bengio. Adversarial machine learning at scale. *arXiv preprint arXiv:1611.01236*, 2016. 1, 2
- [46] Alexey Kurakin, Ian J Goodfellow, and Samy Bengio. Adversarial examples in the physical world. In *Artificial intelligence safety and security*, pages 99–112. Chapman and Hall/CRC, 2018. 1
- [47] Cassidy Laidlaw, Sahil Singla, and Soheil Feizi. Perceptual adversarial robustness: Defense against unseen threat models. In *International Conference on Learning Representations*, 2021. 2
- [48] Minjong Lee and Dongwoo Kim. Robust evaluation of diffusion-based adversarial purification. In *Proceedings of the IEEE/CVF International Conference on Computer Vision*, pages 134–144, 2023. 2

- [49] Xuechen Li, Ting-Kam Leonard Wong, Ricky T. Q. Chen, and David Duvenaud. Scalable gradients for stochastic differential equations. *International Conference on Artificial Intelligence and Statistics*, 2020. 5
- [50] Xiao Li, Wenxuan Sun, Huanran Chen, Qiongxu Li, Yingzhe He, Jie Shi, and Xiaolin Hu. Adversarial diffusion bridge model for reliable adversarial purification. In *The Thirteenth International Conference on Learning Representations*, 2025. 2
- [51] Xiu-Chuan Li, Xu-Yao Zhang, Fei Yin, and Cheng-Lin Liu. F-mixup: Attack cnns from fourier perspective. In *2020 25th International Conference on Pattern Recognition (ICPR)*, pages 541–548. IEEE, 2021. 1
- [52] Guang Lin, Chao Li, Jianhai Zhang, Toshihisa Tanaka, and Qibin Zhao. Adversarial training on purification (ATop): Advancing both robustness and generalization. In *The Twelfth International Conference on Learning Representations*, 2024. 2
- [53] Guang Lin, Zerui Tao, Jianhai Zhang, Toshihisa Tanaka, and Qibin Zhao. Adversarial guided diffusion models for adversarial purification, 2024. 2
- [54] Ze Liu, Yutong Lin, Yue Cao, Han Hu, Yixuan Wei, Zheng Zhang, Stephen Lin, and Baining Guo. Swin transformer: Hierarchical vision transformer using shifted windows. In *Proceedings of the IEEE/CVF international conference on computer vision*, pages 10012–10022, 2021. 3, 5
- [55] Bo Luo, Yannan Liu, Lingxiao Wei, and Qiang Xu. Towards imperceptible and robust adversarial example attacks against neural networks. In *Proceedings of the AAAI conference on artificial intelligence*, 2018. 1
- [56] Cheng Luo, Qinliang Lin, Weicheng Xie, Bizhu Wu, Jinheng Xie, and Linlin Shen. Frequency-driven imperceptible adversarial attack on semantic similarity. In *Proceedings of the IEEE/CVF conference on computer vision and pattern recognition*, pages 15315–15324, 2022. 1
- [57] Xinsong Ma, Zekai Wang, and Weiwei Liu. On the tradeoff between robustness and fairness. *Advances in Neural Information Processing Systems*, 35:26230–26241, 2022. 2
- [58] Aleksander Madry, Aleksandar Makelov, Ludwig Schmidt, Dimitris Tsipras, and Adrian Vladu. Towards deep learning models resistant to adversarial attacks. *arXiv preprint arXiv:1706.06083*, 2017. 1, 2
- [59] Jan Hendrik Metzen, Tim Genewein, Volker Fischer, and Bastian Bischoff. On detecting adversarial perturbations. *arXiv preprint arXiv:1702.04267*, 2017. 2
- [60] Yichuan Mo, Dongxian Wu, Yifei Wang, Yiwen Guo, and Yisen Wang. When adversarial training meets vision transformers: Recipes from training to architecture. *Advances in Neural Information Processing Systems*, 35:18599–18611, 2022. 5, 6
- [61] Apostolos Modas, Seyed-Mohsen Moosavi-Dezfooli, and Pascal Frossard. Sparsefool: a few pixels make a big difference. In *Proceedings of the IEEE/CVF conference on computer vision and pattern recognition*, pages 9087–9096, 2019. 1
- [62] Omar Montasser, Steve Hanneke, and Nathan Srebro. Adversarially robust learning with unknown perturbation sets. In *Conference on Learning Theory*, pages 3452–3482. PMLR, 2021. 2
- [63] Seyed-Mohsen Moosavi-Dezfooli, Alhussein Fawzi, and Pascal Frossard. Deepfool: a simple and accurate method to fool deep neural networks. In *Proceedings of the IEEE conference on computer vision and pattern recognition*, pages 2574–2582, 2016. 1, 2
- [64] Alexander Quinn Nichol and Prafulla Dhariwal. Improved denoising diffusion probabilistic models. In *International conference on machine learning*, pages 8162–8171. PMLR, 2021. 4
- [65] Weili Nie, Brandon Guo, Yujia Huang, Chaowei Xiao, Arash Vahdat, and Anima Anandkumar. Diffusion models for adversarial purification. In *International conference on machine learning*. PMLR, 2022. 2, 4, 5, 6
- [66] OpenAI. Guided diffusion library. <https://github.com/openai/guided-diffusion>, 2021. 5
- [67] Tianyu Pang, Chao Du, Yinpeng Dong, and Jun Zhu. Towards robust detection of adversarial examples. *Advances in neural information processing systems*, 31, 2018. 2
- [68] Nicolas Papernot, Patrick McDaniel, Xi Wu, Somesh Jha, and Ananthram Swami. Distillation as a defense to adversarial perturbations against deep neural networks. In *2016 IEEE symposium on security and privacy (SP)*, pages 582–597. IEEE, 2016. 2
- [69] Hadi Salman, Andrew Ilyas, Logan Engstrom, Ashish Kapoor, and Aleksander Madry. Do adversarially robust imagenet models transfer better? *Advances in Neural Information Processing Systems*, 33:3533–3545, 2020. 5, 6
- [70] Pouya Samangouei, Maya Kabkab, and Rama Chellappa. Defense-GAN: Protecting classifiers against adversarial attacks using generative models. In *International Conference on Learning Representations*, 2018. 2
- [71] Ali Shahin Shamsabadi, Ricardo Sanchez-Matilla, and Andrea Cavallaro. Colorfool: Semantic adversarial colorization. In *Proceedings of the IEEE/CVF conference on computer vision and pattern recognition*, pages 1151–1160, 2020. 1
- [72] Yash Sharma, Gavin Weiguang Ding, and Marcus Brubaker. On the effectiveness of low frequency perturbations. In *Proceedings of the Twenty-Eighth International Joint Conference on Artificial Intelligence (IJCAI)*, pages 470–478, 2019. 1
- [73] Vasu Singla, Songwei Ge, Basri Ronen, and David Jacobs. Shift invariance can reduce adversarial robustness. *Advances in Neural Information Processing Systems*, 34:1858–1871, 2021. 2
- [74] Jascha Sohl-Dickstein, Eric Weiss, Niru Maheswaranathan, and Surya Ganguli. Deep unsupervised learning using nonequilibrium thermodynamics. In *International conference on machine learning*, pages 2256–2265. pmlr, 2015. 4
- [75] Yang Song and Stefano Ermon. Generative modeling by estimating gradients of the data distribution. *Advances in neural information processing systems*, 32, 2019. 2, 4
- [76] Yang Song, Taesup Kim, Sebastian Nowozin, Stefano Ermon, and Nate Kushman. Pixeldefend: Leveraging generative models to understand and defend against adversarial ex-

- amples. In *International Conference on Learning Representations*, 2018. 2
- [77] Yang Song, Jascha Sohl-Dickstein, Diederik P Kingma, Abhishek Kumar, Stefano Ermon, and Ben Poole. Score-based generative modeling through stochastic differential equations. In *International Conference on Learning Representations*, 2021. 2, 4
- [78] Vignesh Srinivasan, Csaba Rohrer, Arturo Marban, Klaus-Robert Müller, Wojciech Samek, and Shinichi Nakajima. Robustifying models against adversarial attacks by langevin dynamics. *Neural Networks*, 137:1–17, 2021. 2
- [79] David Stutz, Matthias Hein, and Bernt Schiele. Confidence-calibrated adversarial training: Generalizing to unseen attacks. In *International conference on machine learning*, pages 9155–9166. PMLR, 2020. 2
- [80] Christian Szegedy, Wojciech Zaremba, Ilya Sutskever, Joan Bruna, Dumitru Erhan, Ian Goodfellow, and Rob Fergus. Intriguing properties of neural networks. *arXiv preprint arXiv:1312.6199*, 2013. 1
- [81] Hugo Touvron, Andrea Vedaldi, Matthijs Douze, and Hervé Jégou. Fixing the train-test resolution discrepancy. *Advances in neural information processing systems*, 32, 2019. 1
- [82] Florian Tramer and Dan Boneh. Adversarial training and robustness for multiple perturbations. *Advances in neural information processing systems*, 32, 2019. 2
- [83] Florian Tramèr, Alexey Kurakin, Nicolas Papernot, Ian Goodfellow, Dan Boneh, and Patrick McDaniel. Ensemble adversarial training: Attacks and defenses. *arXiv preprint arXiv:1705.07204*, 2017. 2
- [84] Dimitris Tsipras, Shibani Santurkar, Logan Engstrom, Alexander Turner, and Aleksander Madry. Robustness may be at odds with accuracy. In *International Conference on Learning Representations*, 2019. 2, 6
- [85] Aaron Van den Oord, Nal Kalchbrenner, Lasse Espeholt, Oriol Vinyals, Alex Graves, et al. Conditional image generation with pixelcnn decoders. *Advances in neural information processing systems*, 29, 2016. 2
- [86] Jinyi Wang, Zhaoyang Lyu, Duhua Lin, Bo Dai, and Hongfei Fu. Guided diffusion model for adversarial purification. *arXiv preprint arXiv:2205.14969*, 2022. 2
- [87] Zekai Wang, Tianyu Pang, Chao Du, Min Lin, Weiwei Liu, and Shuicheng Yan. Better diffusion models further improve adversarial training. In *International Conference on Machine Learning*, pages 36246–36263. PMLR, 2023. 2
- [88] Dongxian Wu, Shu-Tao Xia, and Yisen Wang. Adversarial weight perturbation helps robust generalization. *Advances in neural information processing systems*, 33:2958–2969, 2020. 2
- [89] Chaowei Xiao, Jun-Yan Zhu, Bo Li, Warren He, Mingyan Liu, and Dawn Song. Spatially transformed adversarial examples. In *International Conference on Learning Representations*, 2018. 1
- [90] Chaowei Xiao, Zhongzhu Chen, Kun Jin, Jiong Xiao Wang, Weili Nie, Mingyan Liu, Anima Anandkumar, Bo Li, and Dawn Song. Densepure: Understanding diffusion models for adversarial robustness. In *The Eleventh International Conference on Learning Representations*, 2023. 2
- [91] Weilin Xu, David Evans, and Yanjun Qi. Feature squeezing: Detecting adversarial examples in deep neural networks. *arXiv preprint arXiv:1704.01155*, 2017. 2
- [92] Jongmin Yoon, Sung Ju Hwang, and Juho Lee. Adversarial purification with score-based generative models. In *International Conference on Machine Learning*, pages 12062–12072. PMLR, 2021. 2
- [93] Runpeng Yu, Songhua Liu, Xingyi Yang, and Xinchao Wang. Distribution shift inversion for out-of-distribution prediction. In *Proceedings of the IEEE/CVF Conference on Computer Vision and Pattern Recognition*, pages 3592–3602, 2023. 2
- [94] Hongyang Zhang, Yaodong Yu, Jiantao Jiao, Eric Xing, Laurent El Ghaoui, and Michael Jordan. Theoretically principled trade-off between robustness and accuracy. In *International conference on machine learning*, pages 7472–7482. PMLR, 2019. 2, 6
- [95] Zhengyu Zhao, Zhuoran Liu, and Martha Larson. Towards large yet imperceptible adversarial image perturbations with perceptual color distance. In *Proceedings of the IEEE/CVF conference on computer vision and pattern recognition*, pages 1039–1048, 2020. 1
- [96] Hegui Zhu, Yuchen Ren, Chong Liu, Xiaoyan Sui, and Libo Zhang. Frequency-based methods for improving the imperceptibility and transferability of adversarial examples. *Applied Soft Computing*, 150:111088, 2024. 1